

## Effect of thin amorphous layers on channeling in diamond

R. W. Fearick, T. E. Derry, and J. P. F. Sellschop

*Schonland Research Centre for Nuclear Sciences, University of the Witwatersrand, Johannesburg, WITS 2050, South Africa*

(Received 13 June 1989)

The minimum yield has been measured for the channeling of 1.0-MeV protons in diamond overlaid with a wide range of thicknesses of amorphous carbon, aluminum, or gold layers. The data have been compared with the predictions of multiple-scattering theory, and good agreement is found. A quartic approximation is introduced to describe the angular yield, which is needed to evaluate the theoretical minimum yield. The use of power-law scaling in the relationship between scattering in different materials is investigated and shown to be useful in the treatment of mixed layers. An approximate expression for the effect on the yield of thin layers is derived and investigated. This expression is useful in the evaluation of the effect of thin contamination layers on crystals.

### I. INTRODUCTION

The channeling of ion beams in crystals is influenced by the presence of amorphous layers on the crystal surface. An initially well-collimated beam is scattered in the layer, and the ions enter the crystal with a distribution of angles relative to the initial direction. The minimum yield, in particular, is sensitive to relatively thin layers.

Several authors<sup>1-4</sup> have investigated the validity of various plural-scattering theories in determining the yield and the energy dependence of the effect. These experiments were a prelude to the study and analysis of radiation damage by channeling measurements, using a plural-scattering model, and, as such, were concerned with layer thicknesses typical of radiation damage layers. The problems of thin impurity layers, as typified by the contamination of the crystal surface by oxide layers or the condensation of vapors from the vacuum system, has received little attention experimentally, although the effects was considered theoretically by Lindhard.<sup>5</sup>

In this paper, the effect on the yield of surface layers evaporated onto diamond crystals is investigated. The use of diamond as a target crystal has allowed scattering in carbon layers to be investigated; carbon is an important constituent of contamination films. In addition, aluminum and gold layers were used. Plural-scattering theory<sup>6</sup> allows the scattering distribution to be expressed as the function of two dimensionless variables, a reduced scattering angle  $\bar{\alpha}$  and a reduced film thickness  $\tau$ , for all ion-film combinations. A wide range of reduced thickness  $\tau$  from  $\tau=0.02$  to  $\tau=150$  has been covered; the significance of  $\tau$  is that it is the mean number of collisions of the ion with the film atoms, with a cross section of  $\pi a^2$ , where  $a$  is the Thomas-Fermi screening radius.

In addition to the plural-scattering distribution, the yield as a function of angle in the bare crystal is required in order to calculate the yield on the covered crystal. A quartic approximation is introduced which gives better results than the usual square-well approximation and approaches the accuracy of the experimentally measured azimuthally averaged yield.<sup>2</sup>

Attention has been paid to the case of thin layers, where the effect on the yield is small, and a theoretical expression is derived, based on the Thomas-Fermi cross section, which gives better results than the Lindhard result,<sup>5</sup> which is based on the Rutherford cross section. As a result of slight oxidation of the aluminum layer, we are led to consider power-law scaling of the yield as a function of thickness, which leads to a method for describing the scattering in mixed layers.

### II. THEORETICAL PRINCIPLES

#### A. Multiple scattering

The plural and multiple scattering of ions in amorphous monatomic layers has been treated by Meyer<sup>7</sup> and by Sigmund and Winterbon<sup>6</sup> using the Thomas-Fermi similarity concepts of Lindhard, Scharff, and Schiøtt.<sup>8</sup> The theory assumes that ions are scattered through small angles in binary collisions and that energy loss may be neglected. The ion-atom potential is assumed to be of the screened-Coulomb type.

The angular distribution  $F(x, \alpha)$  of ions of mass  $M_1$  and atomic number  $Z_1$  after traversing a thickness  $x$  of material of density  $N$ , atomic mass  $M_2$ , and atomic number  $Z_2$  is given by

$$F(x, \alpha) d\Omega = \bar{\alpha} d\bar{\alpha} \int_0^\infty J_0(\bar{\alpha} z) e^{-\tau \Delta(z)} z dz \quad (1)$$

$$\equiv \bar{\alpha} d\bar{\alpha} f_1(\tau, \bar{\alpha}),$$

where

$$\Delta(z) = \int_0^\infty \frac{f(\bar{\phi})}{\bar{\phi}^2} [1 - J_0(z\bar{\phi})] d\bar{\phi}$$

and

$$\tau = \pi a^2 N x, \quad \bar{\alpha} = \frac{E a}{2 Z_1 Z_2 e^2} \alpha.$$

Here  $\alpha$  is the total deflection angle of the beam (assumed small),  $d\Omega$  the solid angle into which the beam is scat-

tered,  $J_0$  is the zero-order Bessel function, and  $a$  is the screening radius associated with the potential.  $f_1(\tau, \bar{\alpha})$  is a universal function describing the scattering for all ion-target combinations as a function of the reduced thickness  $\tau$  and reduced scattering angle  $\bar{\alpha}$ . The function  $f(\bar{\phi})$  is related to the differential scattering cross section which for Thomas-Fermi screened-Coulomb potentials can be approximately expressed as

$$d\sigma = \pi a^2 \frac{d\bar{\phi}}{\bar{\phi}^2} f(\bar{\phi}).$$

The distribution  $f_1(\tau, \bar{\alpha})$  is normalized,

$$\int_0^\infty f_1(\tau, \bar{\alpha}) d\bar{\alpha} = \int_\Omega F(x, \alpha) d\Omega = 1$$

and is tabulated for a wide range of  $\tau$  and  $\bar{\alpha}$  for the Thomas-Fermi and Lenz-Jensen potentials by Sigmund and Winterbon.<sup>6</sup>

In general, Eq. (1) must be evaluated numerically. Some simplification is possible for power-law potentials of the form  $V(r) \sim r^{-1/m}$ . Then

$$f(\bar{\phi}) = \lambda \bar{\phi}^{1-2m}, \quad (2)$$

where  $\lambda$  depends on  $m$ .  $f_1(\tau, \alpha)$  can then be expressed as a power series. The quantity  $\bar{\alpha}^2 f_1(\tau, \bar{\alpha})$  becomes a function of the variable  $\bar{\alpha}^{2m}/c\tau$ , where  $c$  depends on  $m$ . This scaling can be approximately extended to the Thomas-Fermi case as Eq. (2) approximates the Thomas-Fermi cross section rather well over limited regions of  $\bar{\phi}$  according to the value of  $m$ . This has been exploited by Marwick and Sigmund<sup>9</sup> who matched  $f_1(\tau, 0)$  for the power potential to the corresponding quantity for the Thomas-Fermi potential and obtained an effective power  $m = m(\tau)$  for a thickness  $\tau$ . The Thomas-Fermi scattering distribution could then be well approximated by the series expansion of  $f_1(\tau, \bar{\alpha})$  for the power  $m$ , leading to a great simplification in the evaluation of  $f_1(\tau, \bar{\alpha})$ .

### B. Yield in channeling measurements

In the usual elastic backscattering arrangement of a channeling measurement, the normalized yield  $\chi(\psi, \phi)$  near an axial direction depends on both the polar angle  $\psi$  from the axial direction and the azimuthal angle  $\phi$  measured from some reference plane. When the beam, aligned in an axial direction, is scattered in an amorphous layer of thickness  $x$  deposited on the crystal surface, it enters the crystal with some distribution  $F(x, \psi)$  and the yield becomes

$$\chi_L = \int F(x, \psi) \chi(\psi, \phi) d\Omega$$

(where  $L$  indicates the surface layer).

Integrating over the azimuthal angle and assuming the scattering angles to be small, the yield becomes

$$\chi_L(x) = 2\pi \int_0^\infty F(x, \psi) \chi(\psi) \psi d\psi,$$

where  $\chi(\psi)$  is the azimuthally averaged yield on the uncovered crystal for incidence angle  $\psi$ . The yield may be written in reduced units as

$$\chi_L(\tau) = \int_0^\infty f_1(\tau, \bar{\alpha}) \chi(\bar{\alpha}) \bar{\alpha} d\bar{\alpha}. \quad (3)$$

Thus the yield for a beam aligned with the axis of a crystal covered with an amorphous layer may be determined by using the appropriate multiple-scattering distribution together with the experimentally determined azimuthally averaged yield. The yield is commonly observed to vary with depth in the crystal—the above procedure may be used to find the yield at any depth, by using the appropriate depth-dependent  $\chi(\bar{\alpha})$ .

In practice, the measurement of the azimuthally averaged yield can be complicated and time consuming, especially, if, as in our case, the goniometer in which the crystal is mounted has only two angular degrees of freedom. Some approximate form of  $\chi(\bar{\alpha})$  then becomes inviting. In this paper, two approximations are investigated, a square-well approximation, first introduced by Lugujo and Mayer,<sup>2</sup> and a quartic approximation.

The square-well approximation is

$$\chi(\psi) = \begin{cases} \chi_{\min}, & \psi < \psi_{1/2} \\ 1, & \psi \geq \psi_{1/2} \end{cases},$$

The yield on a crystal with a surface layer then becomes in reduced units,

$$\chi_L(\tau) = \chi_{\min} + (1 - \chi_{\min}) P(\bar{\alpha}_{1/2}, \tau),$$

where

$$P(\bar{\alpha}_{1/2}, \tau) = \int_{\bar{\alpha}_{1/2}}^\infty f_1(\tau, \bar{\alpha}) d\bar{\alpha}$$

and  $\bar{\alpha}_{1/2}$  is the reduced  $\psi_{1/2}$ .

This approximation can be expected to underestimate the yield, especially if the width of the multiple-scattering distribution is of the same order as  $\psi_{1/2}$ . In this case the extra weight given by the exact  $\chi(\psi)$  in the region  $0 < \psi < \psi_{1/2}$  will be important. For this reason we introduce a quartic approximation which gives a reasonably good approximation to  $\chi(\psi)$  in the region  $\psi < \psi_{1/2}$  (at least at small depths). This approximation is

$$\chi(\psi) = \begin{cases} \chi_{\min} + (1 - \chi_{\min}) \frac{1}{2} \left[ \frac{\psi}{\psi_{1/2}} \right]^4, & \psi < \sqrt{2} \psi_{1/2} \\ 1, & \psi > \sqrt{2} \psi_{1/2} \end{cases}.$$

### C. Power-law scaling

For power-law cross sections the function  $\bar{\alpha}^2 f_1(\tau, \bar{\alpha})$  becomes a function of the single variable  $\bar{\alpha}^{2m}/c\tau$ . Thus for a constant  $m$  the yield in the covered crystal, calculated from the corresponding power-law multiple scattering is a function of  $\bar{\alpha}_{1/2}/(c\tau)^{1/2m}$ . In the Thomas-Fermi case no such scaling exists. However, the equivalent power  $m(\tau)$  remains approximately constant over limited ranges of  $\tau$ , varying most rapidly in the region  $0.1 \leq \tau \leq 10$ . In these regions where  $m$  is only varying slowly, approximate scaling of the yield can be expected. Inasmuch as the Thomas-Fermi cross section is a good approximation to reality, similar scaling can be expected for the experimental results over appropriate regions of  $\tau$ . In order to investigate this, the quantity  $(c\tau)^{1/2m}$  was evaluated as a function of  $\tau$ , by matching the value of

$f_1(\tau, \bar{\alpha})$  for the Thomas-Fermi potential, as tabulated by Sigmund and Winterbon, to the power-law value,

$$f_{1P}(\tau, 0) = \frac{\Gamma(1/m)}{2m(c\tau)^{(1/m)},}$$

where  $\Gamma(x)$  is the gamma function. Thus,

$$(c\tau)^{1/2m} = \left[ \frac{\Gamma(1/m)}{2mf_{1P}(\tau, 0)} \right]^{1/2}.$$

The quantity  $(c\tau)^{1/2m}$  is shown as a function of  $\tau$  in Fig. 1.

If such approximate scaling for the yield as a function of  $\tau$  holds, then for equal yields on two substances  $A$  and  $B$ ,

$$\left[ \frac{(c\tau)^{1/2m}}{\bar{\alpha}_{1/2}} \right]_A = \left[ \frac{(c\tau)^{1/2m}}{\bar{\alpha}_{1/2}} \right]_B.$$

Thus a thickness of one material may be transformed into an equivalent thickness of another material. This forms the basis of a method for determining the scattering in mixed layers, by transforming the thicknesses of the substances into the equivalent thickness of a common material. The physical assumption in applying this method is that the shape of the multiple-scattering distribution does not change much with  $\tau$ . A similar scaling has been considered by Schmaus *et al.*<sup>10</sup> in the multiple scattering in silicon dioxide layers; however, they apply the scaling to the distribution rather than the yield. In this work, the method is applied to correct the aluminum thickness for a small amount of oxygen contamination.

#### D. Thin impurity layers

The effect of thin impurity layers on the yield has not received much attention, in spite of the fact that contamination buildup on the crystal surface is a common problem, and it is desirable to know the effect on the yield. Clearly, the results of the above sections can be applied.

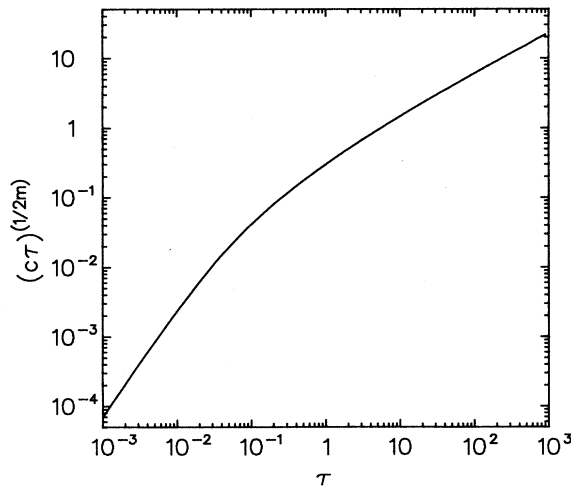


FIG. 1. Graph of  $(c\tau)^{1/2m}$  against  $\tau$  from match of power law to the Thomas-Fermi potential.

However, some simplification is possible for thin layers. Using the Rutherford scattering cross section, Lindhard<sup>5</sup> obtained a result ( $\chi_3$ ) for the contribution to the yield of a thin impurity layer of atomic number  $Z_2$  and areal density  $Nx$ ,

$$\Delta\chi = \chi_3 = \pi Nx \left[ \frac{Z_1 Z_2 e^2}{E} \right]^2 \frac{1}{\psi_{1/2}^2}. \quad (4)$$

This result leads to a useful rule of thumb. The quantity  $Nx$  can be determined from the area  $A$  of the corresponding peak in the backscattering spectrum,  $Nx \propto A/\sigma$ , where  $\sigma$  is the scattering cross section. If the cross section is Rutherfordian, and  $M_1 \ll M_2$ , then

$$\sigma \propto \left[ \frac{Z_1 Z_2 e^2}{E} \right]^2 \csc^4 \frac{\theta}{2},$$

where  $\theta$  is scattering angle in the laboratory frame. It then follows that

$$\chi_3 \propto \frac{A}{\psi_{1/2}^2 \sin^4(\theta/2)},$$

i.e., the increase in yield is proportional to the total integrated impurity count, and is independent of the nature of the impurity.

In general, the screening of the potential becomes important for small-angle scattering, and the Rutherford result is no longer useful. For thin layers the multiple-scattering distribution approaches the single scattering cross section; in reduced units

$$\lim_{\tau \rightarrow 0} \frac{\bar{\alpha}^3}{\tau} f_1(\tau, \bar{\alpha}) = f(\bar{\alpha}), \quad \bar{\alpha} \neq 0.$$

We therefore take for thin layers

$$f_1(\tau, \bar{\alpha}) \approx \frac{\tau}{\bar{\alpha}^3} f(\bar{\alpha}).$$

For large  $\bar{\alpha}$ ,  $f(\bar{\alpha}) \approx 1/2\bar{\alpha}$  and with the square-well approximation,

$$\begin{aligned} \Delta\chi = \chi - \chi_{\min} &= (1 - \chi_{\min}) \frac{\tau}{4\bar{\alpha}^2_{1/2}} \\ &\approx \frac{\tau}{4\bar{\alpha}^2_{1/2}}, \end{aligned} \quad (4')$$

which is the Lindhard result in reduced units.

For heavy surface layer atoms  $\bar{\alpha}_{1/2}$  becomes small. In order to find a more general result, the quartic approximation was applied to a piecewise approximation to the Thomas-Fermi cross section

$$f(\bar{\alpha}) = \begin{cases} \frac{1}{2\bar{\alpha}}, & \bar{\alpha} \geq 1.53 \\ 0.327, & 0.156 \leq \bar{\alpha} \leq 1.53 \\ 1.309\bar{\alpha}^{1/3}, & \bar{\alpha} < 0.156. \end{cases}$$

Then

$$\Delta\chi = [1 - \chi_{\min}] P(\bar{\alpha}_{1/2}, \tau), \quad (5)$$

where

$$P(\bar{\alpha}_{1/2}, \tau) = \begin{cases} \left[ \frac{0.349}{\bar{\alpha}_{1/2}^{2/3}} + 20.8 \right] \tau, & \bar{\alpha}_{1/2} < 0.0131 \\ \left[ \frac{0.367}{\bar{\alpha}_{1/2}} - 0.107 - \frac{2.06 \times 10^{-8}}{\bar{\alpha}_{1/2}^4} \right] \tau, & 0.0131 \leq \bar{\alpha}_{1/2} \leq 1.29 \\ \left[ \frac{0.354}{\bar{\alpha}_{1/2}^2} - \frac{0.098}{\bar{\alpha}_{1/2}^4} \right] \tau, & \bar{\alpha}_{1/2} > 1.29 \end{cases}$$

### III. EXPERIMENTAL

#### A. Apparatus and techniques

Natural diamond crystals selected<sup>11</sup> for low defect levels were cleaned and polished<sup>12</sup> to obtain a flat surface. Gold, aluminum, or carbon layers were evaporated onto the surfaces using standard techniques.

1.0-MeV protons obtained from a pressurized Cockcroft-Walton accelerator were channeled along a  $\langle 110 \rangle$  axis of the crystal at room temperature. Backscattered protons were detected at  $155^\circ$  and spectra were recorded in the usual fashion with an overall energy resolution of 15 keV. The 50-mm<sup>2</sup> detector was masked with a 6-mm aperture. The solid angle subtended was measured with a calibrated <sup>241</sup>Am source and was found to be 4.08 msr, in agreement with the value calculated from geometry. The incident beam was collimated to an angle of 0.001 rad. Beam currents were of the order of 3 nA on a 1-mm<sup>2</sup> spot, and spectra were recorded for an incident charge of 1.2  $\mu$ C. The entire target chamber was insulated and used as a Faraday cup. A copper shield cooled with liquid-nitrogen surrounded the target which was mounted on a two-axis goniometer. Condensation of vapors on the target, as judged from the backscattering spectra, was negligible. The target chamber was pumped with a turbopump and the pressure was about  $10^{-6}$  torr.

The layer thickness was obtained from the backscatter spectrum, as discussed in Sec. III B. After a measurement had been made at a given layer thickness, the crystal was rotated to face an ion sputtering gun mounted in the chamber, and a portion of the layer was removed by sputtering with 900-eV argon ions. Another spectrum was then recorded and the process was repeated until the layer had been removed. No argon retention in the layer was observed. As judged from the shape of the backscattering spectrum, the layer was removed uniformly. There was no anomalous angular dependence of the layer thickness for any material, and the layers were taken to be amorphous for the purposes of the experiment.

#### B. Determination of layer thickness

The layer thickness was determined from the backscattering spectrum with the usual relationship

$$Nx = \frac{A}{n_i \sigma \delta \Omega},$$

where  $Nx$  is the areal density of the layer,  $A$  is the num-

ber of counts in the appropriate peak of the spectrum,  $n_i$  is the number of incident protons,  $\delta \Omega$  is the solid angle subtended by the detector and  $\sigma$  is the differential cross section for scattering into the solid angle. The integration of the gold or aluminum peaks was simple as the peaks were well separated from any interfering peaks and the background was low. The aluminum was accompanied by a small quantity of oxygen and the oxygen peak was also integrated for later inclusion in the total layer thickness. The peak due to the carbon layer was separated from the bulk diamond spectrum graphically, as illustrated in Fig. 2. The error introduced by this procedure was estimated from various possibilities of drawing the lines as about 5%.

The Rutherford cross section was used for scattering of the protons from aluminum and gold. For aluminum the cross section, while essentially Rutherfordian,<sup>13</sup> does have a narrow resonance at 991.9 keV with a width of about 100 eV. The cross section is enhanced by about 15% just above the resonance energy and decreased by 15% just below it.<sup>14</sup> The maximum error that could be incurred by the neglect of the resonance was estimated at 1% for protons leaving the layer at the resonance energy. For exit energies away from the resonance energy, the shape of the resonance assured that the effect on the measured layer thickness was negligible. Tabulated stopping powers<sup>15</sup> indicated that in no cases did the protons leave

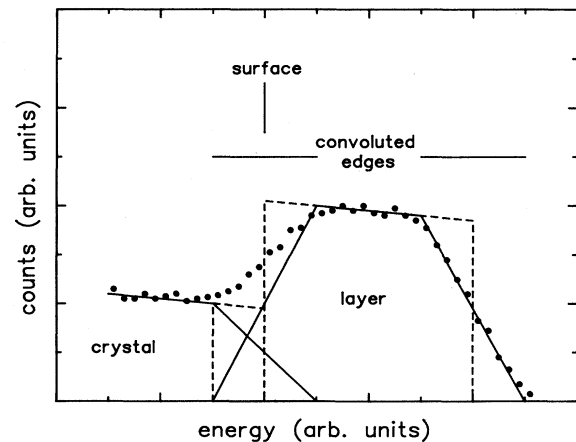


FIG. 2. Graphical separation of carbon layer contribution to the backscattering spectrum, from that of the crystal.

the layer in the resonance region, and the effect of the resonance was thus neglected.

The cross sections for carbon<sup>16</sup> and oxygen<sup>17</sup> were interpolated from measured values, the accuracy being 5% for carbon and 20% for oxygen. The large uncertainty in the case of oxygen has little effect as the oxygen thickness was only a small correction to the aluminum thickness.

The energy dependence of the cross section was taken into account for the aluminum layer, the mean energy of protons in the layer being estimated from the tabulated stopping power. The maximum deviation of the cross section from the 1.000-MeV value was 1.7%. For other cross sections, the 1.000-MeV values were used for all layer thicknesses: For carbon and oxygen, the cross sections vary slowly with energy in the regions considered, and any correction would be much smaller than the uncertainty in the measured cross section; for gold, the energy loss in the layer never exceeded 3 keV and any correction would be less than 0.3%.

For convenient comparison with experimental results obtained from the multiple-scattering theory of Sigmund and Winterbon, the layer thickness was calculated in terms of the reduced thickness  $\tau$ . The oxygen value was scaled to an equivalent thickness of aluminum, according to the results of Sec. II D, and was included in the total  $\tau$  value for aluminum. The correction to the aluminum reduced thickness ranged from 3% for the thickest aluminum layer to 12% for the thinnest.

### C. Determination of the minimum yield

The minimum yield was determined by plotting the spectrum and extrapolating a smooth curve drawn through points to the position of the surface. The surface was taken to be at that energy corresponding to halfway up the step in the interface between the carbon layer and the diamond, or halfway down the edge of the diamond spectrum for gold and aluminum, or if the yield was sufficiently low for there to be a well-developed surface peak, at the peak position.

The yield thus determined was normalized to the random yield, using a random spectrum measured on the uncovered diamond, but dividing by the value of the random spectrum at the energy corresponding to the surface of the covered crystal. The yield should be determined using a random spectrum measured with the same layer thickness as the channeled spectrum: In order to minimize radiation damage to the crystal this was not done. The above procedure is equivalent to using a random spectrum covered by a carbon layer which gives the same energy loss as the actual layer on the diamond. For the carbon layer the procedure is satisfactory (with the neglect of any possible small alloptropic effect on the stopping power). The energy loss through the gold layer was sufficiently small that any errors due to the procedure were negligible. In the case of the aluminum layers, the procedure was estimated to give a maximum error in the random surface position of about 10 keV, or two channels of the spectrum. The systematic variation in random level over this interval was much less than the statistical uncertainty in the spectrum and was thus ignored.

## IV. RESULTS AND DISCUSSION

### A. Power-law scaling

The yield for the three cases, carbon, aluminum, and gold, was evaluated as a function of  $(c\tau)^{1/2m}/\bar{\alpha}_{1/2}$  and is plotted in Fig. 3. The results shown for aluminum do not contain the oxygen correction, which is rather smaller than the spread in values in Fig. 3. The three elements, while falling on their own distinct curves, are grouped closely. Values of  $m(\tau)$  vary from about 0.4 (for gold) to 0.85 (for carbon) but an approximate scaling is clearly observed. This scaling is better for the cases of aluminum and carbon where the range of  $m(\tau)$  is from 0.55 to 0.85. A universal curve is sketched in Fig. 3 which describes the three cases to an accuracy of about 30%.

The observation of this scaling indicated that it was reasonable to use the procedure outlined in Sec. II C to correct the aluminum values for oxygen, although some error can be expected. Correction and combination of layers can be expected to be quite accurate, however, in cases where the values of  $m(\tau)$  for individual components are of the same order.

### B. Minimum yield: Results

The measured  $\langle 110 \rangle$  minimum yield at the surface  $\chi_{\min}$  is plotted as a function of  $\tau$  for the three cases, carbon, aluminum, and gold, in Figs. 4, 5, and 6, respectively, together with the theoretical curve. The errors shown include, for  $\tau$ , the various errors and approximations mentioned in Sec. III, together with the error in layer thickness from the counting statistics. The error in the yield is estimated from a consideration of various possibilities in extrapolation of the yield to the surface and includes the effect of errors in the random spectrum. The thicknesses for aluminum include the contribution from oxygen.

The theoretical curves have been calculated using the Thomas-Fermi multiple-scattering distributions of Sig-

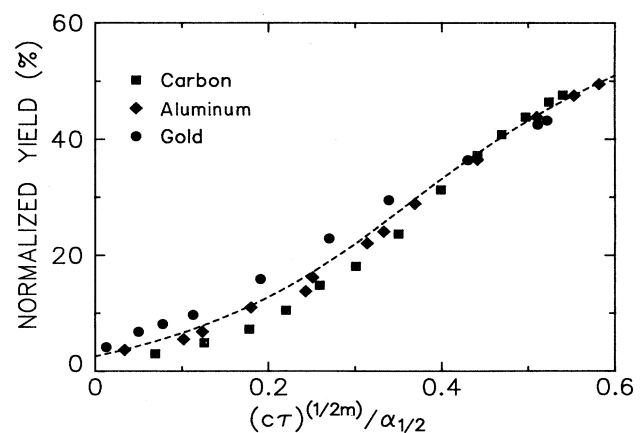
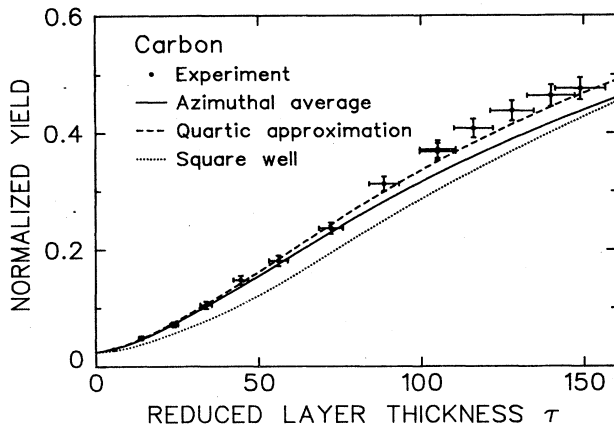
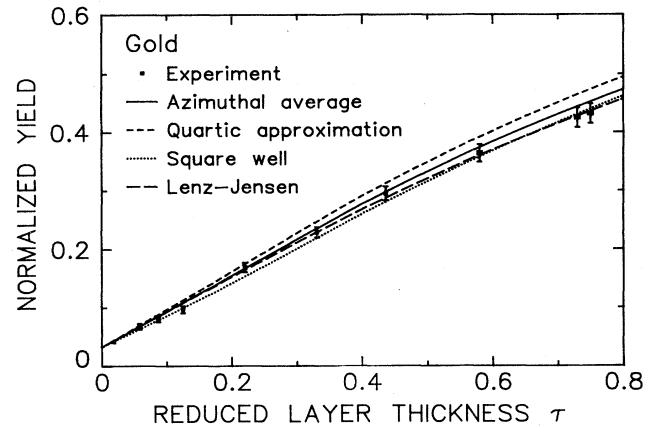


FIG. 3. Yield for all experimental points measured, plotted as a function of the power-law variable  $(c\tau)^{1/2m}/\bar{\alpha}_{1/2}$ . The dashed line gives an approximate universal curve for the determination of the minimum yield due to a surface layer.

FIG. 4. Minimum yield as a function of  $\tau$  for carbon layer.FIG. 6. Minimum yield as a function of  $\tau$  for gold layer.

mund and Winterbon. Three different angular yield functions have been used and are shown in Fig. 7. These are as following:

(i) the experimentally obtained azimuthally averaged yield, measured on an uncovered crystal by averaging the yield obtained at  $5^\circ$  steps over  $90^\circ$  in azimuth, from a  $\{100\}$  to a  $\{110\}$  plane. The two-axis design of the goniometer necessitated the simultaneous variation of both coordinates in order to scan along a path at a constant angular offset from the  $\langle 110 \rangle$  axis. The critical angle measured agrees with the result of Derry *et al.*<sup>18</sup>

(ii) the square-well approximation,

(iii) the quartic approximation. These approximations were used with the minimum yield measured on the uncovered crystal before the start of each set of experiments.

The integral in Eq. (3) is in terms of the reduced scattering angle  $\bar{\alpha}$  which is energy dependent. The appropriate energy is the average energy of the beam in the layer where the scattering takes place; this may be written as  $E_0 - \frac{1}{2}\Delta E$ , where  $E_0$  is the initial energy and  $\Delta E$  is the energy loss in the layer. This is a good approxima-

tion for thin layers. The critical angle  $\psi_{1/2}$  which, in the form  $\bar{\alpha}_{1/2}$ , defines the scale of  $\chi(\bar{\alpha})$  in Eq. (3) is also energy dependent, varying as  $E^{-1/2}$ . The appropriate energy for this angle is  $E_0 - \Delta E$ . However,

$$\begin{aligned}\bar{\alpha}_{1/2}(E_0 - \Delta E) &= \frac{a}{2Z_1 Z_2 e^2} (E_0 - \frac{1}{2}\Delta E) \psi_{1/2}(E_0 - \Delta E) \\ &\approx \frac{a}{Z_1 Z_2 e^2} E_0 \psi_{1/2}(E_0) \\ &= \bar{\alpha}_{1/2}(E_0)\end{aligned}$$

for small  $\Delta E$ , so that, for the critical angle, the energy loss in the layer may be neglected to a good approximation.

The multiple-scattering distributions tabulated by Sigmund and Winterbon<sup>5</sup> were fitted with a rational function which gave the same large-angle behavior as the tabulated functions, i.e.,  $\sim \tau/\bar{\alpha}^4$ , and the integration was performed numerically. The resulting theoretical points were used with spline interpolation to produce the lines of Figs. 4-6.

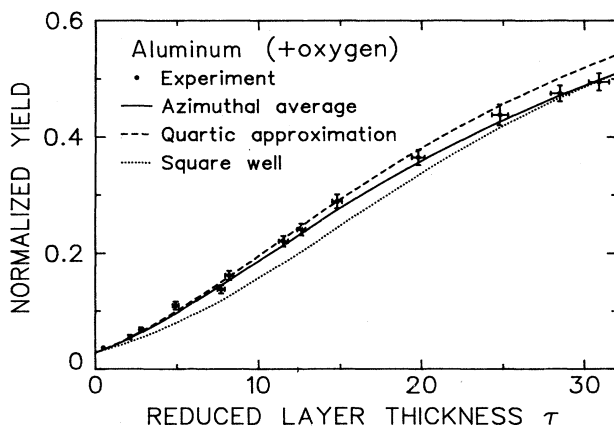
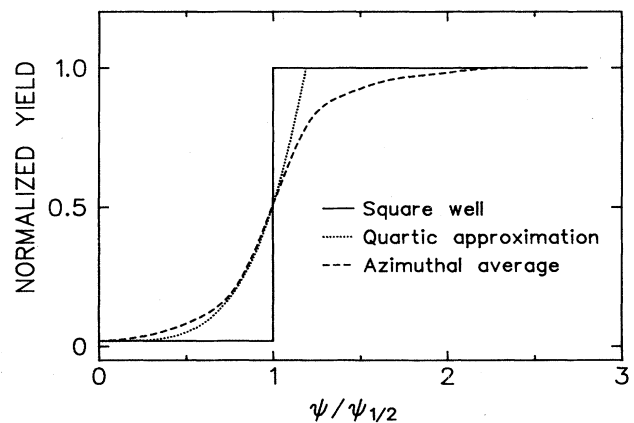
FIG. 5. Minimum yield as a function of  $\tau$  for aluminum layer.

FIG. 7. Angular yield functions used for theoretical calculations of the minimum yield, as described in the text.

### C. Minimum yield: Discussion

The theoretical curves based on the averaged angular yield are seen to be in agreement with experiment to within 10%, the greatest discrepancy being for carbon. The two approximations also give reasonable results, especially the quartic approximation at lower yields.

For carbon, the quartic approximation is in closest agreement with the experimental results. This might indicate that the angular yield function needs to be closer to the quartic shape. However, this is not reflected in the other results and there is no reason to expect that the angular yield profile should depend on the nature of the layer. Another possible explanation of the discrepancy is the uncertainty in the cross section: It does not seem possible to explain all the discrepancy on this basis, especially as the fractional deviation increases with increasing  $\tau$ . This could only be accounted for with rather drastic variations in the energy dependence of the cross section. A more likely explanation is that an interatomic potential based on Thomas-Fermi statistical considerations is not strictly applicable between light atoms with few electrons (carbon) and protons. It is also possible that some effect of the nuclear potential is being felt by the protons. The results indicate that a potential with rather less screening than the Thomas-Fermi potential would be appropriate: This would allow more scattering and result in a higher yield. Bernhard *et al.*,<sup>19</sup> in measuring the multiple scattering of protons of energies up to 270 keV through thin carbon foils and analyzing the results using Meyer's theory,<sup>7</sup> have found that a screening length of 28.8 pm is consistent with their data, rather than the value of 25.8 pm used here. This increase in screening length does decrease the screening, but insufficiently to explain our result. Nevertheless, the agreement between theory and experiment for carbon must be regarded as satisfactory, bearing in mind the simplicity of the Thomas-Fermi scattering theory which provides a universal description of all target-ion pairs.

For the other two layer materials, agreement of theory with experiment is found to be good. This agrees with the results obtained by other authors<sup>1,2</sup> with silicon crystals, and extends these results to yields below 15% which were not measured by those authors. We note that in the case of the aluminum layer, this good agreement is partly the result of including a small correction due to the presence of oxygen according to the procedure of Sec. II C.

At higher layer thickness, the experimental points for gold fall below the theoretical curve and agree most closely with the square-well approximation, although the deviation is rather small. Calculations were made using the multiple-scattering distribution for the Lenz-Jensen potential and are also shown in Fig. 6. The agreement is better than with the Thomas-Fermi distribution. The difference between the Thomas-Fermi and Lenz-Jensen distributions becomes smaller as the reduced thickness  $\tau$  is increased and the yield curves for the two potentials in the case of aluminum and carbon are very close. For gold, the difference between the two curves and the experimental results is barely significant considering the errors; however, it might indicate that the Lenz-Jensen po-

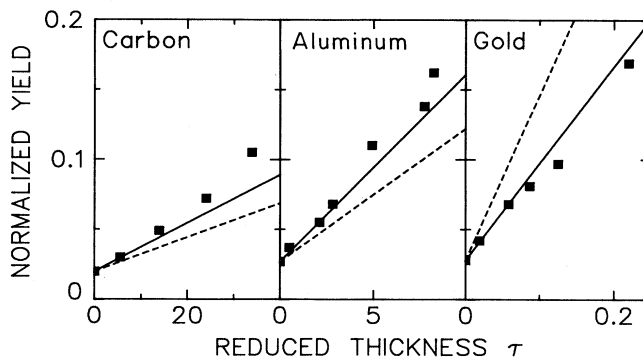


FIG. 8. Minimum for thin layers. The dashed line gives the prediction of the Lindhard theory, Eq. (4), while the full line gives the prediction of Eq. (5).

tential is more appropriate for small-angle proton-gold scattering.

### D. Yield for thin layers

The experimental results of the surface yield measurements for thin layers, that is, for small increases of the yield, are plotted in Fig. 8. Also plotted are the theoretical results from Eqs. (4) and (5). It is apparent that Lindhard's expression gives only a rough approximation to the yield. The expression is best at intermediate  $\bar{\alpha}_{1/2}$  where the rise in the Rutherford cross section above the Thomas-Fermi cross section compensates to some extent for the low  $\bar{\alpha}$  component included by using a yield function with nonzero weight between 0 and  $\bar{\alpha}_{1/2}$ .

The expression given in Eq. (5) agrees more closely with experiment for increases in the yield of several percent. Comparison with Figs. 4–6 suggests that it may be used to give estimates of the yield up to quite large layer thicknesses. Some improvement in accuracy can be obtained by using a closer approximation to  $f(\bar{\alpha})$  than the piecewise approximation, for example, that due to Winterbon *et al.* (WSS).<sup>20</sup> The simplicity of the approach will be lost, however, as numerical integration will then be required for the evaluation of Eq. (3).

## V. CONCLUSIONS

The results show that satisfactory agreement can be obtained between the theoretically calculated yields and the experimentally measured yields, using azimuthally averaged yields. The quartic approximation introduced here also gives good results, especially for lower layer thicknesses. The results indicate that high accuracy and precision experiments of this type will be able to distinguish between different interaction potentials used in the calculation of multiple-scattering distributions. For lower layer thicknesses, an expression based on single scattering in the Thomas-Fermi approximation has been found, that gives good agreement with the measurements: This should be especially useful in the evaluation of the effect of contamination layers on the minimum yield.

### ACKNOWLEDGMENTS

The authors acknowledge with appreciation the support of the Foundation for Research Development and of de Beers Industrial Diamonds (Pty) Ltd.

- <sup>1</sup>E. Rimini, E. Lugujo, and J. W. Mayer, *Phys. Rev. B* **6**, 718 (1972).
- <sup>2</sup>E. Lugujo and J. W. Mayer, *Phys. Rev. B* **7**, 1782 (1973).
- <sup>3</sup>S. U. Campisano, G. Foti, F. Grasso, and E. Rimini, *Phys. Rev. B* **8**, 1811 (1973).
- <sup>4</sup>G. Götz, K. Hehl, F. Schwabe, and E. Glaser, *Radiat. Eff.* **25**, 27 (1975).
- <sup>5</sup>J. Lindhard, *K. Dansk. Vidensk Selsk. Mat. Fys. Medd.* **4**, 34 (1965).
- <sup>6</sup>P. Sigmund and K. B. Winterbon, *Nucl. Instrum. Methods* **119**, 541 (1974).
- <sup>7</sup>L. Meyer, *Phys. Status Solidi B* **44**, 253 (1971).
- <sup>8</sup>J. Lindhard, M. Scharff, and H. E. Schiøtt, *K. Dansk. Vidensk Selsk. Mat. Fys. Medd.* **10**, 36 (1968).
- <sup>9</sup>A. D. Marwick and P. Sigmund, *Nucl. Instrum. Methods* **126**, 317 (1975).
- <sup>10</sup>D. Schmaus, F. Abel, M. Bruneaux, C. Cohen, A. L'Hoir, G. Della Mea, A. V. Drigo, S. Lo Russo, and G.G. Bentini, *Phys. Rev. B* **19**, 5581 (1979).
- <sup>11</sup>R. W. Fearick, T. E. Derry, and J. P. F. Sellschop, *Nucl. Instrum. Methods* **168**, 195 (1980).
- <sup>12</sup>M. Rebak, J. P. F. Sellschop, T. E. Derry, and R. W. Fearick, *Nucl. Instrum. Methods* **167**, 115 (1979).
- <sup>13</sup>T. Awaya, *J. Phys. Soc. Jpn.* **20**, 669 (1965).
- <sup>14</sup>R. S. Bender, F. C. Shoemaker, S. G. Kauffmann, and G. M. B. Bouricius, *Phys. Rev.* **76**, (1949).
- <sup>15</sup>H. H. Andersen and J. Ziegler, *Hydrogen Stopping Powers and Ranges in all Elements* (Pergamon, New York, 1977).
- <sup>16</sup>H. L. Jackson, A. I. Galonsky, F. J. Epling, R. W. Hill, E. Goldberg, and J. R. Cameron, *Phys. Rev.* **89**, 365 (1952).
- <sup>17</sup>R. A. Laubenstein, M. J. W. Laubenstein, L. J. Koester, and R. C. Mobley, *Phys. Rev.* **84**, 12 (1951).
- <sup>18</sup>T. E. Derry, R. W. Fearick, and J. P. F. Sellschop, *Phys. Rev. B* **26**, 17 (1982).
- <sup>19</sup>F. Bernhard, P. Krygel, R. Manns, and S. Schwabe, *Radiat. Eff.* **13**, 249 (1972).
- <sup>20</sup>K. B. Winterbon, P. Sigmund, and J. B. Sanders, *K. Dansk. Vidensk Selsk. Mat. Fys. Medd.* **14**, 36 (1970).